CHAPTER III

ROLE OF PRIMARY AMINE IN POLYOXYMETHYLENE (POM) /BENTONITE NANOCOMPOSITE FORMATION **

Thontree Kongkhlang [a], Yasushi Kousaka [b], Toshikazu Umemura [b], Daigo Nakaya [c],

Wandee Thuamthong [c], Yupin Pattamamongkolchai [c], Suwabun Chirachanchai [a,*]

[a] *The Petroleum and Petrochemical College, Chulalongkorn University, Chula Soi 12, Phyathai Road, Pathumwan, Bangkok 10330, Thailand*
[b] *Mitsubishi Gas Chemical Company, Mitsubishi Building 5-2, Marunouchi 2-chome, Chiyoda-ku, Tokyo 100-8324, Japan*
[c] *Thai Polyacetal Co., Ltd., Padaeng Industrial Estate, 1 Padaeng Road, Map-Ta-Phut, Rayong 21150, Thailand*

*Corresponding author

ABSTRACT

Polyoxymethylene (POM)/organo-modified bentonite nanocomposites are successfully prepared by melt intercalation method of which a primary ammonium salt is an effective surfactant, as evidenced from improvement in mechanical and gas barrier properties. Nanocomposite structures analyzed by XRD and TEM show mixed nanostructure of flocculation and exfoliation (flocculated/exfoliated nanocomposite) when primary ammonium-treated bentonite is used, whereas the quaternary ammonium-treated bentonites induce the mixture of intercalation and flocculation (intercalated/flocculated nanocomposite). The incorporation of organo-modified bentonite gives an effect on crystallization by generating numerous nucleating sites, especially in the case of bentonite with primary ammonium

surfactant. The nanocomposites obtained exhibit improvement in flexural strength, flexural modulus, and elongation at break. The thermal degradation temperature is decreased by 40 °C, whereas the oxygen barrier is increased by 50%, as compared to neat POM.

1. Introduction

For decades, organic-inorganic nanocomposites have attracted great interest from researchers due to the synergistic effects of the two components close to the molecular level. The incorporation of a few percentages of layered silicate fillers into the polymer matrix brings significant increases in stiffness, strength, and heat resistance [1], together with decreases in flammability [2,3], gas impermeability [2], and moisture absorption [4], as compared to micro- and macroscale polymer composites. Silicate layers or clays such as montmorillonite, hectorite, and bentonite have been comprehensively considered in more detail, for example, aspect ratio, ionic strength, orientation, and intercalation of the polymer matrix [1,5,6]. Various polymers, especially polyimide [7,8]. epoxy resin [9,10], polystyrene [11], polycaprolactone [12], acrylic polymer [13], and polyolefin [14], were reported for successful polymer/clay nanocomposites.

Polyacetal (polyoxymethylene, POM) is one of the major engineering thermoplastics commonly used to replace metal or alloy products such as gears. bushings, etc., owing to its high stiffness, dimensional stability, and corrosion resistance. However, low impact toughness, sensitivity to notch, and low heat-resistance limit its range of applications. The development of POM by various strategies, for example, copolymerizing with oxyethylene chain [15,16], blending with elastomers [17,18], etc.. are proposed in the past. The hybridization with inorganic fillers. especially organoclay, to form nanocomposites is another approach to improve the properties of POM from the nano-scale structure. It should be noted that as POM under thermal treatment tends to degrade and consequently generate

formaldehyde, the blending or mixing under thermal treatment with avoidance of the degradation has to be considered.

Although the success of POM/organoclay nanocomposites may bring about an improvement in physical and mechanical properties of POM, such as impact toughness, heat distortion resistance, gas barrier property, only a few reports are on this theme. Xu et al. studied the nonisothermal crystallization kinetics of POM/montmorillonite (MMT) in which the crystallization rate was found to be faster than that of the neat POM at a given cooling rate [19]. Pielichowski and Leszczynska reported the mixed tactoid-exfoliated structure and the mechanical properties of POM/MMT nanocomposites [20]. Despite the fact that the preparation of POM/organoclay nanocomposite has been reported, the studies on the factors related to the nanocomposite formation are not included.
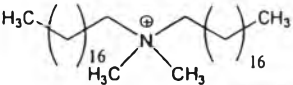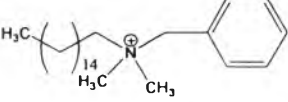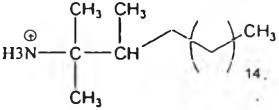
Based on the above viewpoint, we pay our attention on (i) the effect of surfactant on giving a favorable organoclay layer for POM intercalation, (ii) the effects of organoclay on the physical and mechanical properties of POM/organoclay nanocomposites, (iii) the thermal stability of POM/organoclay nanocomposites, and (iv) the rheological properties of POM/ organoclay nanocomposites.

2. Experimental

2.1 Materials

Polyoxymethylene (POM) with a dioxalane (DOL) content of 4.4% was supplied by Thai Polyacetal Co. Ltd., Thailand, and was used as received. Organically modified bentonites $[M_xMg)_6Si_{8-x}Ca_x(Si_8O_{20})OH)_4]$ with different alkylamine surfactants (Table 3.1) were supplied by Süd Chemie (Germany) and Kunimine Industries (Japan).

Table 3.1 Bentonite based organo-modified clays used in the present work

Organoclay	Company	Surfactant
NF5	Sud Chem	
NF9	Sud Chem	
KT	Kunimine Industries	

2.2 Instruments and Equipment

The packing structure was studied by a Rigaku RINT 2000 wide angle X-ray diffractometer (WAXD) with CuK_α as the X-ray source, a scanning angle of 1.5-10° 2θ, operating at 40 kV, 30 mA, and equipped with a Ni filter. A Perkin Elmer Pyris Diamond TG-DTA and a Perkin Elmer DSC7 were applied under N_2 with a flow rate of 20 mL/min and a heating rate of 10°C/min from -20°C to 200°C. The degree of crystallinity (χ_c) was estimated by assuming that the heat of melting per unit mass of crystalline material is identical to that of melting of a 100% crystalline POM sample (i.e. 317.93 J/g, Iguchi et al.[22]). An H-7100 Hitachi transmission electron microscope was used to observe the POM/bentonite samples and the observation was done under the courtesy of Sumitomo Rubber Co. Ltd. The samples were prepared using a Reichert Ultra cut cryo-ultramicrotome without staining. A Leica DMRXP polarizing optical microscope (Leica Imaging Systems Ltd.) equipped with a Mettler Toledo FP82HT hot stage and a COHU CCD camera (COHU Inc.) was used to observe the crystallization. The samples were prepared in 0.5 mm thicknesses by using compression molding (Wabash V50H Press) and were cut to 5×5 mm^2. The samples were melted at 190°C for 5 min before transferring to a hot stage set at the predetermined temperature. The spherulitic growth rate was evaluated based on the spherulite diameter developed with time using a video recording system. Measurements of the spherulite diameter (D) vs time (t) were

performed for more than five different spherulites per experiment, and the growth rates (G = dD/dt) were calculated from the slope of the line fitted to the experimental data at a given crystallization temperature. The differences in crystallite size and crystallite density were quantified by counting the number of crystallites/spherulites in a certain area. Melt rheological studies were performed by using a Rheometrics ARES V6.5.6 equipped with a cone (cone diameter 25 mm and angle 0.04 rad) and plate fixture. The gap was set at 0.051 mm. and the transducer sensitivity was between 0.004–10.00 g cm^{-1}. All experiments were measured using the log frequency-sweep test at a given strain (γ) chosen in the linear viscoelastic regime, where the dynamic moduli are independent from strain. The frequencies used were 0.1 to 100 rad/s. Each measurement was carried out at 200°C and was repeated four times. TG-FTIR measurements were carried out by using a TA TGA-2950 interface with a Thermo Nicolet Nexus 670 Fourier transform infrared spectrophotometer. TG measurements were performed using 10 mg of the sample at a heating rate of 10°C/min under nitrogen. Each spectrum was recorded by FTIR every 30 sec with a resolution of 4 cm^{-1}. The oxygen transmission rate through the POM/clay nanocomposite film was measured according to ASTM D1434 at 25°C using a GDP/E gas permeability tester (Brugger, Germany). The total oxygen transmission rate was normalized with film thickness. An Instron universal testing machine (Model 4320, Instron. Corp., Canton, MA, USA) was used with a cross head speed of 50 mm/min. Test pieces for the flexural tests were obtained from a Nissei Plastic Industrial Co. PS40E2ASE injection molding. Tensile and flexural strength were measured according to ASTM D638 and D790.

2.3 Preparation of nanocomposites

The organo-modified bentonites and POM were preliminary dry-mixed by a high speed mixer (CL-F25, Chyau Long Machinery Co. Ltd., Taiwan) at 1:99, by weight. The mixture was melt extruded by using a JSW Co-rotating TEX30α twin screw extruder operated at 210°C (screw speed = 100 rpm). The pellet obtained was dried under vacuum at 60°C for 24 h before use.

3. Results and Discussion

### 3.1. Effect of amine surfactant on intercalation with clay
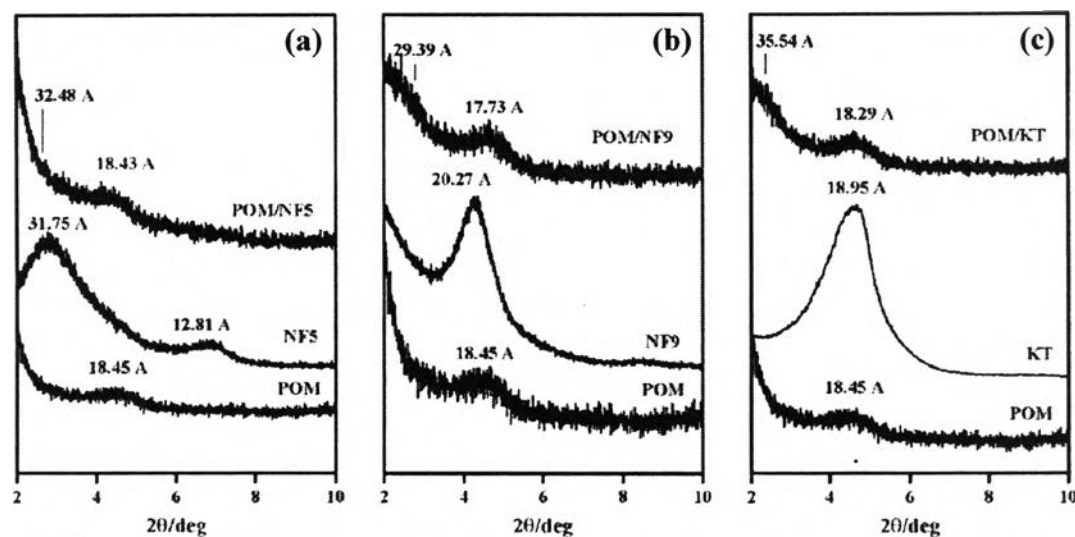
Fig. 3.1. WAXD patterns of (a) POM, NF5, and POM/NF5; (b) POM, NF9, and POM/NF9; (c) POM, KT, and POM/KT.

Fig. 3.1 shows the effect of different amine-treated bentonites on the formation of POM nanocomposites, as observed by WAXD patterns. The interlayer spacing of unmodified bentonite is 12.3 Å [22]. Based on the amine types, NF5 and NF9 were organoclay modified with quaternary ammonium ion, whereas that of KT was the one with primary ammonium ion (Table 3.1). Considering the organoclay, for NF5 and NF9, the diffraction peaks are shifted drastically whereas for KT the diffraction is shifted slightly to the lower 2θ as compared with unmodified bentonite. This indicates the significant intercalation of the quaternary ammonium salt in bentonite silicate layers.

When the organoclay was blended with POM, the diffraction peaks were as follows: for POM/NF5, they are at d-spacing = 18.43 Å and 32.48 Å; for POM/NF9, they are at d-spacing = 17.73 Å and 29.39 Å; for POM/KT, they are at d-spacing = 18.29 Å and 35.54 Å. This implies that the silicate layers are successfully intercalated by the POM chain and generate intercalated nanocomposite structures. It

is noteworthy that the crystalline phase of the POM chain still remains in the system, as evidenced from the remaining diffraction peak at d-spacing = 18.45 Å, especially in the case of POM/NF5. This implies that the crystalline phase of POM is maintained even though the melt blending of nanocomposite preparation was applied; in other words, the POM chain might be well arranged in-between the silicate layers.
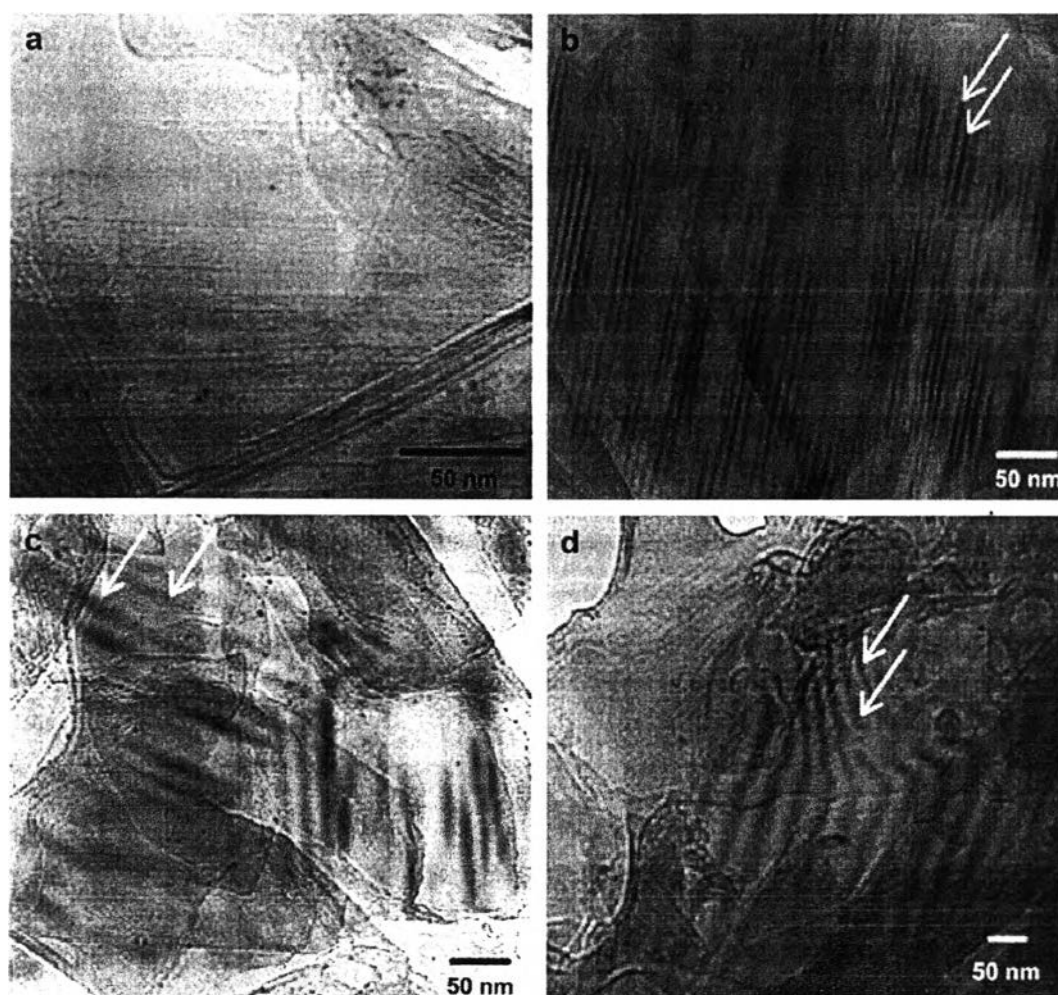
Fig. 3.2. TEM micrographs of (a) POM, (b) POM/NF5, (c) POM/NF9, and (d) POM/KT. Arrows indicate silicate layers in the samples.

Fig. 3.2 shows the TEM micrographs of POM. POM/NF5, POM/NF9, and POM/KT, which confirm our above speculation. In the case of POM/NF5. silicate layers are in the layered structure, as evidenced from the regularly aligned lines with

an interlayer distance of about 3 nm or less (b). The edge-to-edge interaction of the silicate layers is observed, indicating a flocculated nanostructure of POM/NF5. It is important to note that the distance between the silicate layers is constant and well organized. This means that the POM chain is well packed between the silicate layers. The result agrees well with the remaining diffraction peak at d-spacing = 18.43 Å, as mentioned earlier. For POM/NF9, the interlayer distance is about 8 nm or less, and several clay layers are still agglomerated (c). On the other hand, the POM/KT nanocomposite (d) shows that the interlayer distance of the silicate layer is more than 20 nm where the silicates are in a layer-by-layer structure. A similar TEM micrograph was claimed to be an exfoliated nanostructure, as the clay layers were separated with an interlayer distance of more than 20 nm in the case of epoxy/clay nanocomposite as reported by Kong and Park [23]. Thus, in our case, POM/KT possibly is an exfoliated nanocomposite. The edge-to-edge interaction is also observed in the case of POM/NF9 and POM/KT, meaning a flocculated nanocomposite.

Taking the WAXD and TEM results into consideration, it can be concluded that the primary amine treated with bentonite induced the flocculated/exfoliated nanostructure, whereas the quaternary amine-treated bentonite induced the intercalated/flocculated nanostructure.

3.2. Effect of modified bentonite on crystallization properties

As crystallization is involved with physical and mechanical properties, the crystalline morphology and radial spherulitic growth rates of neat POM and POM/organo-modified bentonite nanocomposites are important and therefore are observed by optical microscope. Fig. 3.3 shows representative data of isothermal crystal morphology at 138 °C belonging to the neat POM and POM/KT. For the neat POM. the spherulitic formation was found to grow constantly (a) until the spherulites overlap each other (b). The spherulite forms in circular shape, implying an isotropic (spherical) three-dimensional shape. For the POM/KT system ((c) and (d)), the crystallite sizes are much smaller than the ones from the neat POM. A significant increase in the number of nucleations and the consequent small crystallite formation

are observed. This implies that the dispersed clays function as a nucleating agent when POM started crystallization, as reported in the case of PEO/MMT [24]. Moreover, the crystal morphology is nonspherulitic, implying an anisotropic crystal growth. A similar crystal morphology and crystallization behavior to POM/KT was also observed in the case of POM/NF5 and POM/NF9 nanocomposites.
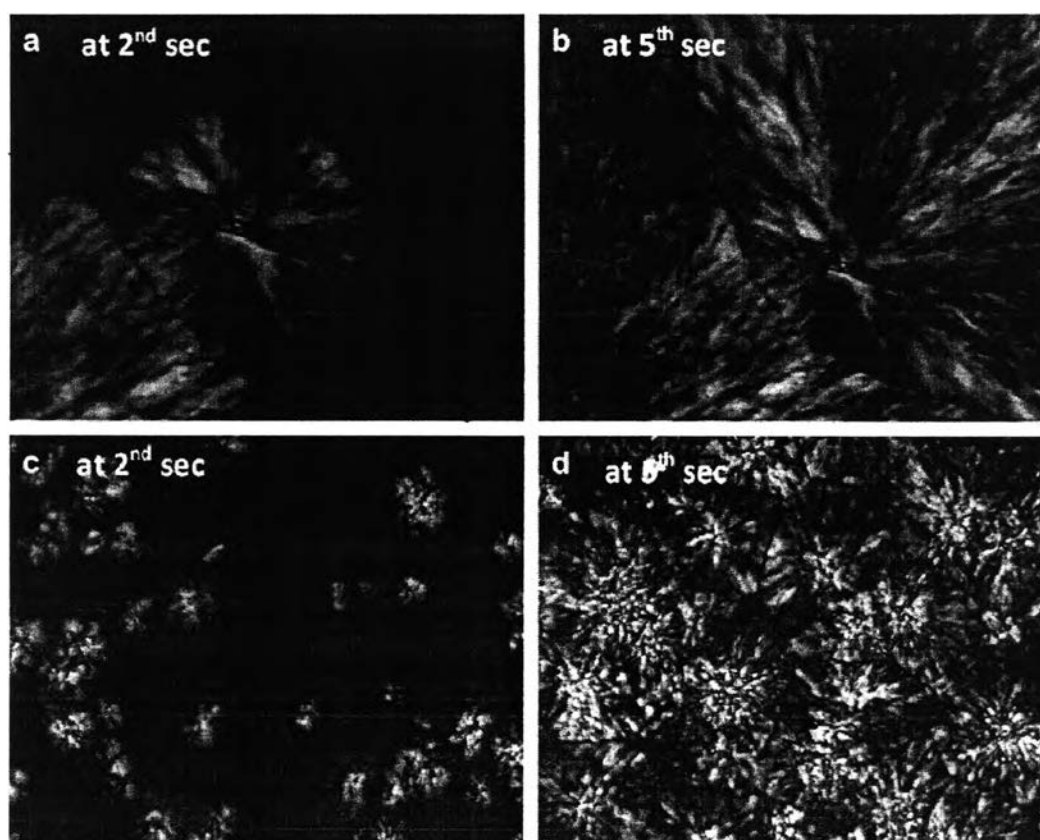
Fig. 3.3. Polarizing optical micrographs of crystallized (at 138 °C) neat POM (a,b) and POM/KT (c,d) at early crystallization stage (a,c) and final crystallization stage (b,d).

Fig. 3.4 shows the number of nucleations and crystallization growth rate of POM for each POM/organo-modified bentonite nanocomposites. The amount of nucleation is increased more than 10 times when organo-modified clays were introduced into the POM matrix, especially in the case of POM/KT (50 times). At the same time, the crystallite growth rate is significantly decreased after POM was intercalated with the organobentonite. The slow crystallization rate might be due to

the hindrance effect of the polymer in the vicinity of silicate, which forces the spherulite to grow around the dispersed silicate layers. Strawhecker and Manias carried out a comparative study of crystallization behavior between the neat PEO and the PEO/Na^+ MMT hybrid to find that the presence of Na^+ MMT inhibited the crystallization of PEO, resulting in a decrease of crystallization growth and crystallization temperature [24]. At that time, lamellar pathways were found to grow around the tactoid of MMT, losing the symmetrical crystallite formation. The delay of crystallization in the region downfield from the tactoid was also observed. In our case, similar results were obtained. For example, the onset crystallization temperatures were shifted to lower values (1-2 °C) in the case of POM/organo-modified bentonite nanocomposites (Table 3.3). This reduction confirmed that the crystallization process was obstructed by the addition of silicate layers. There, an excessive undercooling to initiate the crystallization process might be needed. Table 3.3 also shows that the degree of crystallinity of the POM/organo-modified bentonite nanocomposites decreases as compared to that of the neat POM. It is important to note that the usual crystallization behavior of semicrystalline polymers, such as poly(vinylalcohol) [25], polypropylene [26,27], and nylon 6 [28], containing fillers will normally result in heterogeneous nucleation, promoting crystals in their vicinity. Strawhecker and Manias proposed that the unusual crystallization behavior observed in the case of PEO was a consequence of the coordination between PEO chains and Na^+, adopting conformations with crown-ether arrangements, resulting in highly amorphous structure [24]. Taking this to our consideration, it might be possible that there will be interaction between POM and the remaining trace amount of small cations, i.e. Na^+, leading to amorphous structure in the vicinity of the silicate. It should be recalled that our POM contains 4.4% of oxyethylene unit, which favors the coordinating interaction with metal ion.
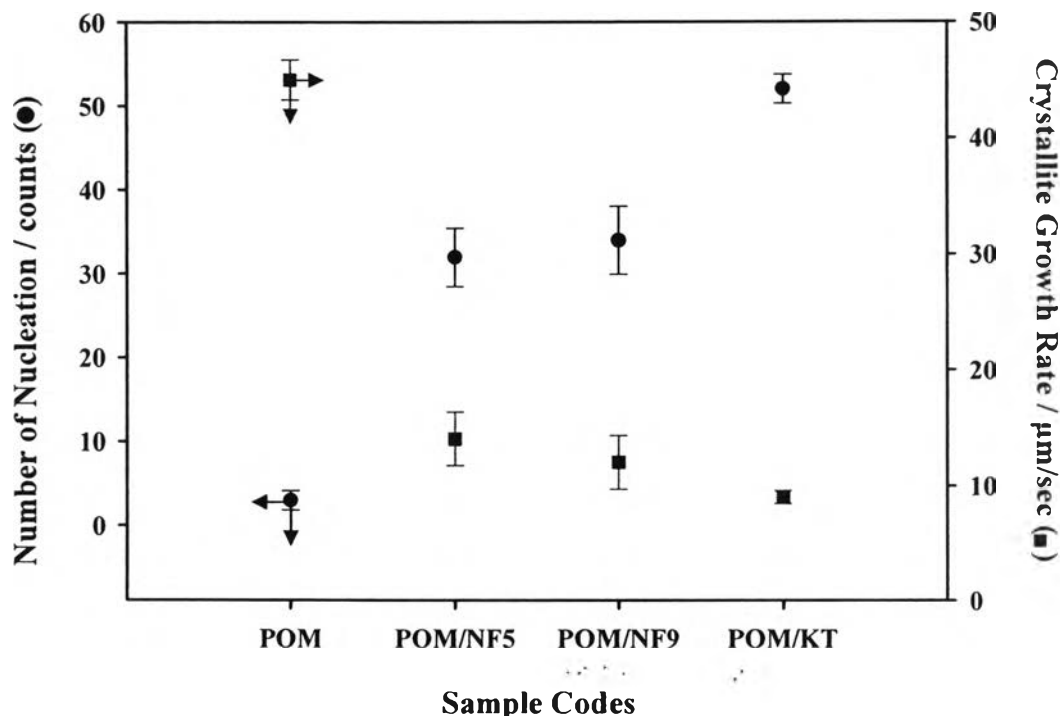
Fig. 3.4. Number of nucleation (●) and crystallite growth rate (■) of POM and POM/organo-modified bentonite nanocomposites.

3.3. Mechanical properties

The mechanical properties of POM/organo-modified bentonite nanocomposites summarized in Table 3.2 are compared to those of the pristine POM. By introducing organo-modified bentonite into the POM matrix, the nanocomposites obtained show a similar tensile strength and flexural modulus to the pristine POM. Flexural strength and elongation at break of those nanocomposites are improved, especially POM/KT. It should be noted that the elongation at break of POM/NF9 is increased up to 25% compared to pristine POM. The flexural strength and elongation at break related to the crystallite density was further studied in order to verify the effect of crystallization behavior on the mechanical properties. Although the elongation at break, flexural strength, and number of nucleation were carried out by

using the different specimen sizes, we neglected the dimension factor since the number of nucleation was obtained from isothermal crystallization at 138 °C.

Table 3.2 Mechanical properties of POM and POM/organo-modified bentonite nanocomposites*

Properties / Units	POM	POM/NF5	POM/NF9	POM/KT
Tensile strength (MPa)	63.0	61.8	62.1	63.1
Elongation at break (%)	27.9	34.7	36.9	32.1
Flexural strength (MPa)	84.6	86.7	86.8	90
Flexural modulus (GPa)	2.28	2.38	2.47	2.56

*average value of ten measurements for each sample is reported with an error ± 2%.

The flexural strength and elongation at break were plotted against the type of POM/modified bentonite-based nanocomposites. Although it is difficult to determine how number of nucleation gives effects to the mechanical properties, an attempt to clarify this was carried out. Fig. 3.5 shows the tendency that the higher the number of nucleation, the increase in both flexural strength and elongation at break will be, even it is not systematically. As shown in Fig. 3.5, when we put the type of the nanocomposites based on the number of nucleation in the graph, the result shows some relationship between the number of nucleation and the mechanical properties, i.e. the higher the number of nucleation, the more the flexural strength and elongation at break. The grain boundary between the crystallites. in other words interspherulite, is believed to play an important role in determining the improvement obtained. It is important to point out that the surfactant used in the POM/KT nanocomposite was a primary amine salt. In other words. the bentonite modified with the primary amine shows improved physical and mechanical properties.
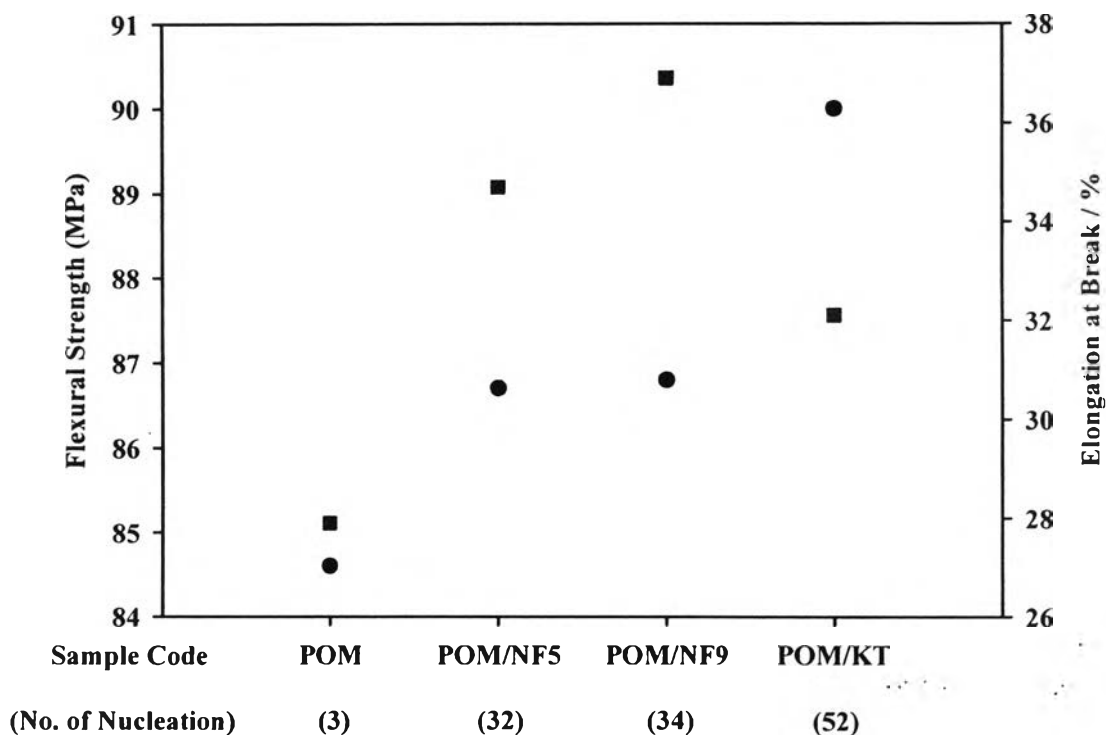
Fig. 3.5. Flexural strength (●) and elongation at break (■) of POM and POM/organo-modified bentonite nanocomposites as a function of number of nucleation. The results are an averaged value from five measurements.

3.4. Rheological properties

Fig. 3.6 shows the frequency dependence of the storage modulus (G') measured at 200°C for POM and POM/organo-modified bentonite nanocomposites. The rheological properties of the pristine polymers. PVDF and PMMA, reported by Moussaif and Groeninckx, were almost the same as those obtained from the PVDF/PMMA-unmodified MMT microcomposite, as seen from the frequency dependence of G' [29]. In our case, the rheological properties of the pristine POM and POM/organo-modified bentonite nanocomposites were studied comparatively. The frequency dependence of G' for the pristine POM and POM/organo-modified bentonite nanocomposites exhibits the normal response of polymer, with a liquid-like behavior at low frequencies (below 1 rad/s). At the same range (below 1 rad/s),

POM/organo-modified clay nanocomposites are found to be more elastic than that of the pristine POM. This might be related to the reinforcing effect from the organo-modified bentonite. However, POM/organo-modifiedbentonite nanocomposites showed less solid-like behavior than that of POM as observed at high frequencies (10-100 rad/s). We suspected that the tactoids (clay crystallites) consisting of intercalated silicate platelets, as well as the individual silicate layers, might be difficult to freely rotate and, as a result, the complete relaxation subjected to shear was prevented. This incomplete relaxation was also suggested by Krishnamoorti et al. as an effect of the percolation, which led to the solid-like behavior in the exfoliated nanocomposites [30].
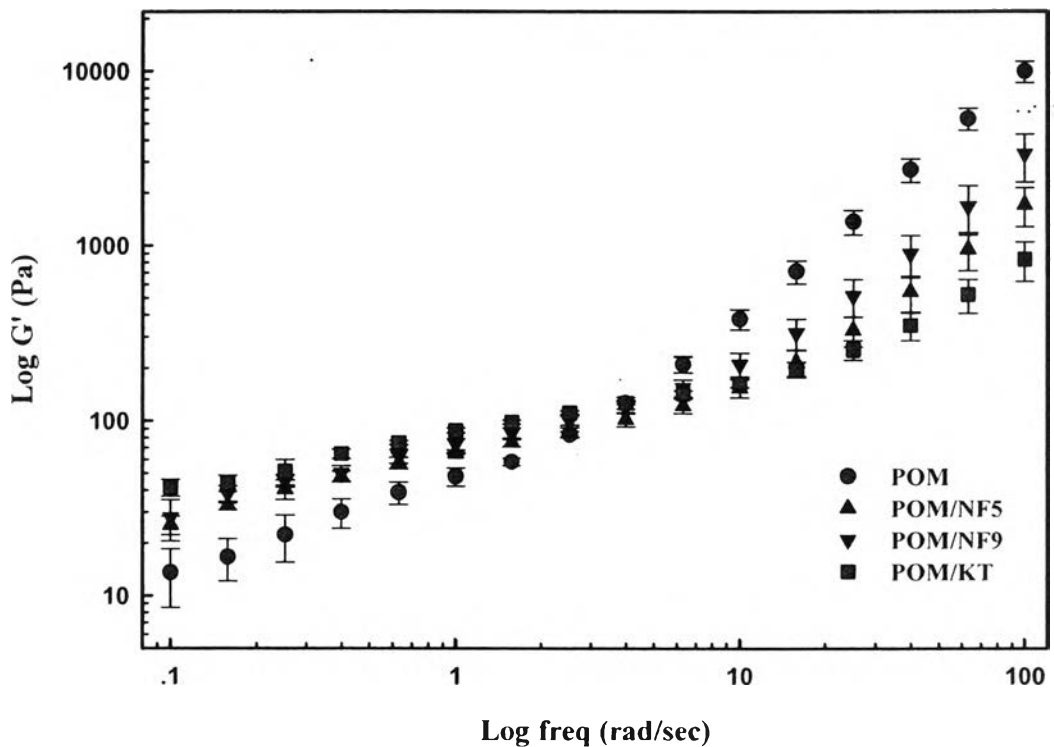

Fig. 3.6. Rheological properties of POM and POM/organo-modified bentonite nanocomposites.

3.5. Thermal properties

The preparation of polymer/organoclay nanocomposites involves the processing temperatures. If the temperature is higher than the thermal stability of the

organic component used for clay modification, decomposition of the polymer may take place [31,32]. Thus, studies on the stability of the polymer in the presence of organoclay to understand the relationship between the molecular structure as well as the thermal stability (decomposition temperature, rate, and the degradation products) of the polymer and organoclay are important. Fig. 3.7 shows the TGA curves of POM and POM/organo-modified bentonite nanocomposites (a) including the TGA and DTG curves of the treated bentonites (b). Unexpectedly, the thermal stability of the POM/organo-modified bentonite nanocomposites is lower than that of the neat POM, especially POM/NF9. It should be noted that the onset degradation of the POM/organo-modified bentonite nanocomposites was at 280 °C; however, at that time, 20% of NF9, 6% of NF5, and 8% of KT were already degraded. Xie et al. reported that the thermal degradation of alkyl ammonium compounds intercalated into MMT galleries was based on the Hoffman mechanism, in which the ammonium cation loses an olefin and an amine, and leaves an acid proton on the surface of the MMT [33]. Here, the degradation of POM might be affected by these acid protons and, as a result, POM/organo-modified bentonite nanocomposites degraded more significantly compared to the neat POM.
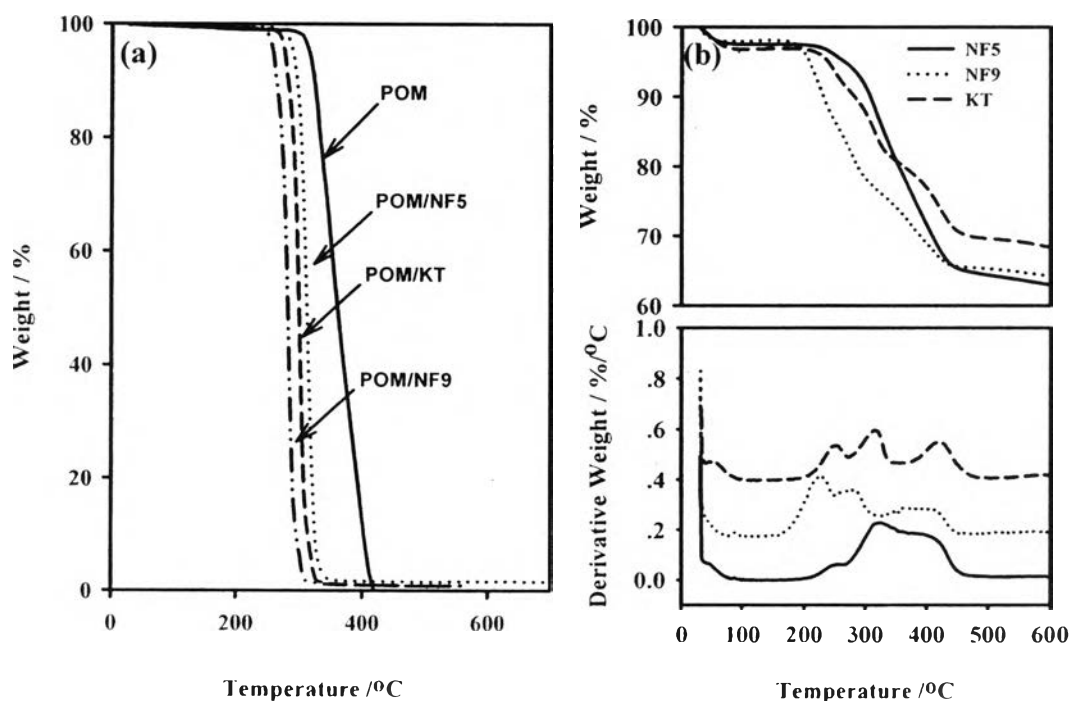
Fig. 3.7. TGA and DTG curves of (a) POM and POM/organo-modified bentonite nanocomposites, and (b) alkyl ammonium-treated bentonite.
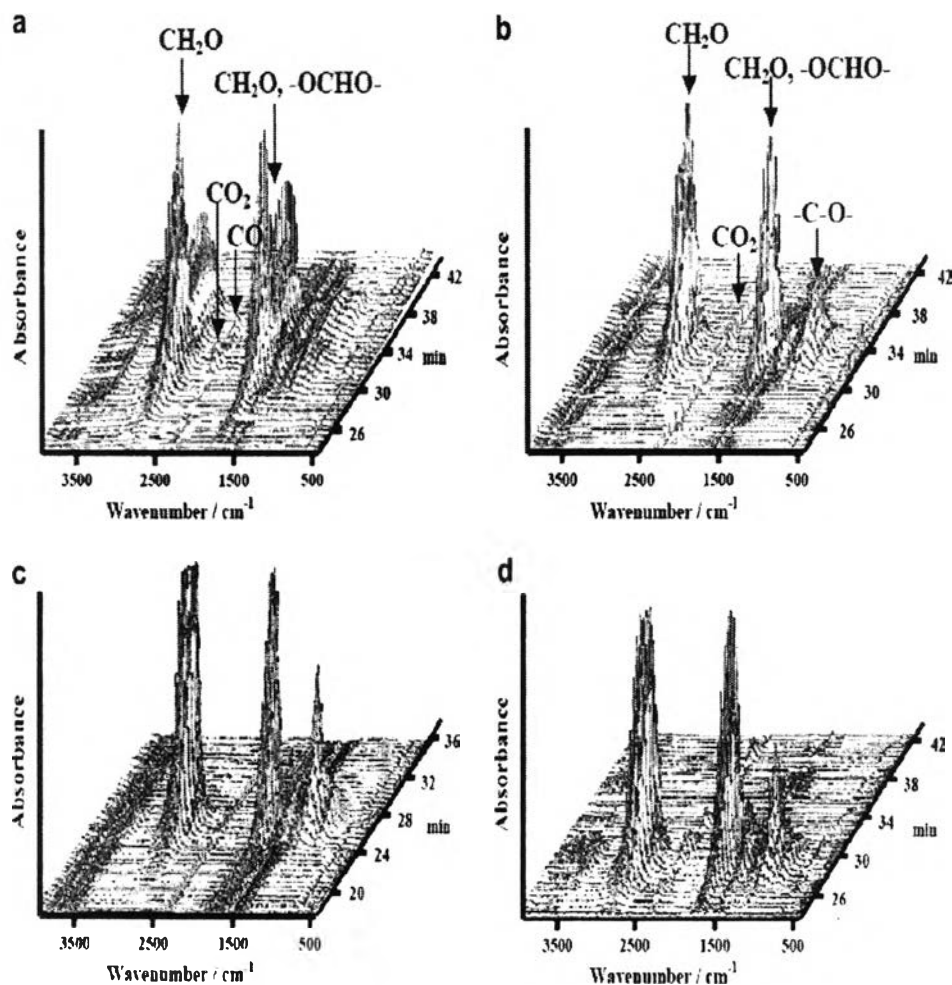
Fig. 3.8. TG-FTIR spectra of gases evolved during thermal degradation of (a) POM,
(b) POM/NF5, (c) POM/NF9, and (d) POM/KT as a function of time.

In order to confirm the degradation, the TG interface with FTIR was applied
(Fig. 3.8). Thermal degradation of POM has also been observed continuously by TG-
FTIR [34]. In the case of neat POM, the degradation occurs at the 30th min and lasts
until the 40th min (a). In the case of POM/NF5, the degradation is similar to that of
the neat POM, i.e. it starts at the 30th min and ends at the 35th min (b). However, for
POM/NF9 and POM/KT, the degradation begins sooner at around 24 min for
POM/NF9 (c) and 26 min for POM/KT (d). The degradation species, as analyzed by
FTIR, are clearly formaldehyde, carbon dioxide, and carbon monoxide, which come

from the depolymerization of chain ends and random chain scission of oxymethylene chain. A remarkable evolution of formaldehyde (H_2CO), observed at the initial stage of degradation and rapidly decomposed for POM/NF9, confirms that the random chain scission of POM is accelerated at elevated temperature. This is relevant to the speculation about the presence of acid protons on the surface of the organo-modified bentonite.

3.6. Gas permeability

The silicate layers are known to increase the gas barrier property by creating a maze or 'tortuous path' that retards the progress of gas molecules through the polymer matrix [1,35,36]. In order to evaluate the permeability of the nanocomposites, here, the oxygen permeability was studied. Table 3.3 shows that the nanocomposite films give a lower oxygen permeability coefficient than the neat POM does. Since the nucleation might influence the gas permeability of the composite films, the effect of the polymer crystallinity on oxygen permeability was compared. The degree of crystallinity (cc) of POM/organo-modified bentonite nanocomposites is slightly lower than that of the neat POM; at the same time, the oxygen permeability of the POM/organo-modified bentonite nanocomposites is reduced as much as 50% as compared to that of the neat POM. Osman et al. reported that there was no direct correlation between the relative permeability and the basal-plane spacing because the tactoids have small aspect ratios and the increase in *d*-spacing decreases it further [4]. However, in our case, a decrease in permeability with increasing d-spacing is observed (Table 3.3). This result might be related to the number of exfoliated layers in the nanocomposite; in other words, the expansion of the d-spacing belonging to the organomodified bentonite obstructs the gas molecule pathways. These results are in accordance with the nanostructure elicited by WAXD and TEM, suggesting the effectiveness of the primary alkyl ammonium compound for the POM/organomodified bentonite-based nanocomposites.

Table 3.3 Thermal properties and O_2 permeability coefficient of POM and POM/bentonite based nanocomposites

Sample	d-spacing (Å)	O_2 permeability coefficient* $(cm^3.mil/m^2.day.bar)$	Thermal and crystallinity properties	
			Onset T_c (°C)	χ_c (%)
POM	18.46	0.65±0.22	146.5	50.0
POM/NF5	32.48 18.43	0.44±0.06	144.9	42.3
POM/NF9	29.39 17.73	0.33±0.05	145.7	49.0
POM/KT	35.54 18.29	0.30±0.02	145.5	47.6

*average of four measurements for each nanocomposite film is reported.

4. Conclusion

Nanocomposite structure is significantly influenced by the surfactant used for bentonite modification. POM/organomodified bentonite nanocomposites showed an intercalated/ flocculated nanostructure when the quaternary ammonium compounds were used. while the primary ammonium compound intercalated bentonite was found to play an important role in the exfoliated POM/organo-modified bentonite nanocomposite formation, which induced an improvement in mechanical and gas barrier properties. The organo-modified bentonites, acting as a nucleating agent, generated numerous nucleating sites with anisotropic crystallite growth. POM/organo-modified clay nanocomposites were found to be more elastic than the pristine POM at low frequency (below 1 rad/s) while showing less elasticity than the pristine POM with frequencies in the range of 10–100 rad/s. The degradation of POM was accelerated by the presence of the organomodified bentonites, owing to the acid protons generated during the thermal degradation of the organo-modified bentonite.

References

[1] Kojima Y, Usuki A, Kawasumi M, Okada A, Kurauchi T, Kamigaito O, et al. Journal of Polymer Science, Part B: Polymer Physics 1994;32:625.

[2] Usuki A, Kawasumi Y, Kojima M, Fukushima Y, Okada A, Kurauchi T, et al. Journal of Materials Research 1993;8:1179.

[3] Zhang J, Wilkie CA. Polymer Degradation and Stability 2003;80:163-9.

[4] Osman MA, Mittal V, Morbidelli M, Suter UW. Macromolecules 2004;37:7250.

[5] Alexandre M, Dubois P. Materials Science and Engineering 2000;28:1.

[6] Sinha Ray S, Okamoto M. Progress in Polymer Science 2003;28:1539.

[7] Yano K, Usuki A, Okada A, Kurauchi T, Kamigaito O. Journal of Polymer Science, Part A: Polymer Chemistry 1993;31:2493.

[8] Delozier DM, Orwoll RA, Cahoon JF, Johnston NJ, Smith Jr JG, Connell JW. Polymer 2002;43:813-22.

[9] Wang MS, Pinnavaia TJ. Chemistry of Materials 1994;6:468.

[10] Giannelis EP. Advanced Materials 1996;8:29.

[11] Aphiwantrakul S, Srikhirin T, Triampo D, Putiworanat R, Limpanart S, Osotchan T, et al. Journal of Applied Polymer Science 2005;95:785e9.

[12] Lepoittevin B, Devalckenaere M, Pantoustier N, Alexandre M, Kubies D, Calberg C, et al. Polymer 2002;43:4017.

[13] Chen Z, Huang C, Liu S, Zhang Y, Gong K. Journal of Applied Polymer Science 2000;75:796.

[14] Hasegawa N, Okamoto H, Kawasumi M, Kato M, Tsukigase A, Usuki A. Macromolecular Materials and Engineering 2000;280/281:76.

[15] Pace-Rodriguez RA. Wang S. Yang NL. Die Makromolekulare Chemie 1990;191:99.

[16] Matsuzaki K. Maeda M. Kondo M. Morishita I, Hamada M, Yamaguchi T, et al. Journal of Polymer Science, Part A: Polymer Chemistry 1997;35:2479.

[17] Chiang WY, Huang CY. Journal of Applied Polymer Science 1989;38:951.

[18] Chiang WY, Huang CY. Journal of Applied Polymer Science 1993;47:105.

[19] Xu W, Ge M, He P. Journal of Applied Polymer Science 2001;82:2281.

[20] Pielichowski K, Leszczynska A. Polimery 2006;51:143.

[21] Iguchi M. Makromolekulare Chemie 1976;177:549e66.

[22] Lee WF, Chen YC. Journal of Applied Polymer Science 2004;91:2934.

[23] Kong D, Park CE. Chemistry of Materials 2003;15:419.

[24] Strawhecker KE, Manias E. Chemistry of Materials 2003;15:844.

[25] Strawhecker K, Manias E. Macromolecules 2001;34:8475.

[26] Maiti P, Nam PH, Okamoto M, Kotaka T, Hasegawa N, Usuki A.
     Macromolecules 2002;35:2042.

[27] Maiti P, Nam PH, Okamoto M, Kotaka T, Hasegawa N, Usuki A. Polymer
     Engineering and Science 2002;42:1864.

[28] Maiti P, Okamoto M. Macromolecular Materials and Engineering
     2003;288:440.

[29] Moussaif N, Groeninckx G. Polymer 2003;44:7899.

[30] Ren J, Silvia AS, Krishnamoorti R. Macromolecules 2000;33:3739.

[31] Leszczy'nska A, Njuguna J, Pielichowski K, Banerjee JR. Thermochimica Acta
     2007;453:75.

[32] Leszczy'nska A, Njuguna J, Pielichowski K, Banerjee JR. Thermochimica Acta
     2007;454:1.

[33] Xie W, Gao Z, Pan WP, Hunter D, Singh A, Vaia R. Chemistry of Materials
     2001;13:2979-90.

[34] Pielichowski K, Leszczyn'ska A. Journal of Thermal Analysis and Calorimetry
     2004;78:631.

[35] Messersmith PB, Giannelis EP. Journal of Polymer Science, Part A: Polymer
     Chemistry 1995;33:1047.

[36] Xu R, Manias E, Snyder AJ, Runt J. Macromolecules 2001;34:337.